Energy Landscape of Two-Dimensional Lattice Polymers†

J. C. Schön

Max-Planck-Institut für Festkörperforschung, Heisenbergstrasse 1, D-70569 Stuttgart, Germany

Received: January 31, 2002; In Final Form: May 6, 2002

The energy landscape of two-dimensional lattice polymers is investigated, using the so-called lid algorithm. We find that a multitude of pockets around local energy minima exist that exhibit approximately exponentially growing local densities of states. This behavior is similar to the energy landscape of e.g. two- and three-dimensional covalent lattice networks and the energy landscape of spin glasses. However, in contrast to these systems, we find that two classes of polymer landscapes exist, depending on the length of the polymers. As a consequence, short polymers appear to show a much more "liquidlike" behavior, while long polymers resemble much more closely the glassy covalent networks.

Introduction

One of the major classes of complex systems that exhibit glassy behavior, such as a glass transition[1,2] or non-Debye relaxations,[3] are the polymers.[4−6] Since they can be synthesized in many well-controlled variations, they have become important from the theoretical point of view as well, serving as a touchstone for many theories and models for glassy or amorphous systems. When trying to find common ground between polymers and the plethora of other complex systems, one needs to abstract on two levels: on one hand, one wishes to concentrate on the general properties of polymers, without getting lost in the details of the specific interaction (the "ideal" polymer), while, on the other hand, one wants to find a bridge that connects the realm of polymers with that of other complex systems, e.g. spin glasses,[7] clusters,[8−10] individual proteins and polymers,[11−14] covalent network glasses,[15] problems in evolution,[16] structure prediction in chemistry,[17,18] or combinatorial optimization problems.[19]

The study of the "ideal" polymer has made great advances in the past decade with the development of lattice polymer models.[20] Here, one no longer tries to account for each individual atom in a polymer—instead one combines several atoms, perhaps even whole side branches of the polymer, into a single building unit. For this unit, an effective interaction both within the polymer (nearest neighbors along the backbone) and with all other polymers is defined. This allows us to concentrate on the abstract polymer and its properties. To allow for the efficient simulation of polymer properties and their dynamical behavior, a second fruitful approximation has been made, i.e., to place these building units on a lattice. In this way, Monte Carlo simulations have become possible that have been used to elucidate much of the behavior of polymers.[21−27]

The bridge that connects these successful abstract models with other complex systems is their energy landscape and its properties;[10,18,28,29] e.g., the relaxation of a system can be visualized as a random walk on the energy landscape of the system, and many low-temperature properties of glasses have been ascribed to certain features of the energy landscape like double-well potentials[30,31] or their extension, the so-called soft potentials.[32,33] However, with current computer resources it is not yet possible to gain a complete picture of the whole landscape of a nontrivial system. Thus, we have concentrated on studying representative subregions of the landscape (called pockets), which are operationally defined as those regions of the energy landscape that can be reached from a local minimum without crossing a sequence of barriers, the so-called lids. This lid algorithm[19,34] has already been successfully applied to several complex systems,[15,19,35,36] and certain features common to all examples have been found, in particular approximately exponentially growing local densities of states and densities of local minima around these pockets.

In this work we present investigations of the application of the lid algorithm to 2D-lattice polymers and compare the results with those found for other complex systems.

Model

The model we use for the 2D-lattice polymers is similar to the bond-fluctuation model employed in MC simulations,[20] where we envision the building units of the polymers to be analogous to carbon atoms connected via covalent bonds. N_p (=1−24) polymers of length l_p (=3−180) were placed on square $S \times S$ 2D lattices ($S = 10-32$) with side lengths $X = Sa$, where a is the spacing of the lattice. $N_A = N_p\, l_p$ is the total number of building units, and $V = S^2$ is the total area of the system in units of a^2. We have performed landscape explorations for 48 different systems (defined by N_p, l_p, and S) covering a large number of densities $\rho = N_A/V$, with up to $N_A = 180$ building units. To simulate an infinite system, periodic boundary conditions were employed.

The lattice constant a was chosen such that the equilibrium distance between two units was on the order of $2a$. In this way, we abstract in this mesoscopic model from the local vibrations and distortions and concentrate on the topological aspects of the polymer configurations instead. Thus, the local densities of state for the pockets in configuration space will represent the excess entropy or so-called configurational entropy of the system—a quantity usually associated with the peak in the specific heat near the glass transition.[5,6]

The interaction potential between neighbors along the polymer consisted of two terms. The first is a radially symmetric two-body term that equals plus infinity for $r < 1.6a$, has a minimum at $\approx 2.2a$, goes to zero at $r = 3.2a$, and equals infinity again for

† Part of the special issue "R. Stephen Berry Festschrift".

10.1021/jp020316o CCC: $22.00
Published on Web 09/12/2002

$r > 3.2a$ (covalent bonds were not allowed to be destroyed!). As a consequence, the maximal allowed density was $\rho_{max} = 1/4$. Second, we employed a three-body term as a function of the angle ($0° \le |\theta| \le 180°$) between units along the polymer, which is infinite for $|\theta| < \theta_0 = 80°$, has a broad minimum at $|\theta| = \theta_{min} = 120°$, and reaches zero smoothly for $|\theta| = 180°$. Choosing $V_3(|\theta| = 180°) = 0$ sets the zero of the energy, while the choices of θ_0 and θ_{min} mimic the preferred bond angle for sp^2-hybridized carbon atoms. If the individual units become very large, one might want to choose different values for θ_0 and θ_{min}, e.g. $\theta_{min} \approx 180°$ for rodlike polymers or $\theta_0 = 0°$ for "floppy" polymers.

The exact functional form of the potential is not critical for the results but is given for completeness (setting $a = 1$):

$$V_2(r) = \begin{cases} +\infty : r < 1.6 \\ 1/3(r-1.6)(r-3.2)^2(r-7.1) : 1.6 \le r \le 3.2 \\ +\infty : r < 3.2 \end{cases} \quad (1)$$

$$V_3(\theta) = \begin{cases} +\infty : |\theta| < \theta_0 = 80° \\ -5.8 \times 10^{-8}(|\theta| - 80)(|\theta| - 180)^2|\theta| : 80° \le |\theta| \le 180° \end{cases} \quad (2)$$

Building units that are not neighbors along a chain only interact via a hard sphere potential, with $V_{HS}(r) = \infty$ for $r < 1.6$ and $V_{HS}(r) = 0$ for $r \ge 1.6$. To focus on the effects most typical for polymers, we did not introduce v. d. Waals or hydrogen bond interactions for nonneighbor building units. (Of course, such terms might prove crucial for the landscape of e.g. proteins and should be included in that case.) Since the configuration space of the lattice polymers is discrete, the landscapes we study are not continuous but instead defined on a so-called metagraph. The connectivity of this metagraph was given by the so-called moveclass: the neighbors of a configuration could be reached by moving one building unit to a neighboring lattice point.

Local minima of the energy landscapes of each of the 48 systems studied were found using simulated annealing, on the average for each system about 20 distinct minima. Overall, over 200 of the corresponding pockets were investigated in detail, with the remaining ones containing too few states to warrant a detailed study ($N(L_{max}) < 10$). (The total computational effort involved was about 2 years on three high-end work stations.) Typical local minimum configurations for a 14×14 lattice are shown in Figure 1. Each of these minima x_i served as a starting point for an exhaustive search using the lid algorithm,[19,34] where for a sequence of energy lids L_k the number of accessible states $N(L_k;x_i)$, accessible minima $M(L_k;x_i)$, local density of states $D(E;L_k,x_i)$, and local density of minima $D_M(E;L_k,x_i)$ were determined. Since the configuration space of the lattice polymers is discrete, each state and minimum inside a pocket around x_i below a lid L could be counted individually.

The size of such a local region in configuration space corresponds to the number of states $N(L_{max})$ that are accessible without crossing a limiting lid L_{max} that connects the pocket to another region of the landscape which contains a configuration with a lower energy. (One can visualize this process by picturing a source of water at x_i. As the water level L rises, neighboring valleys are flooded and the accessible phase space volume $N(L)$ increases, until for $L = L_{max}$ a deeper minimum is found and the process stops.) Due to the periodic boundary conditions of the system, certain configurations were equivalent by symmetry;

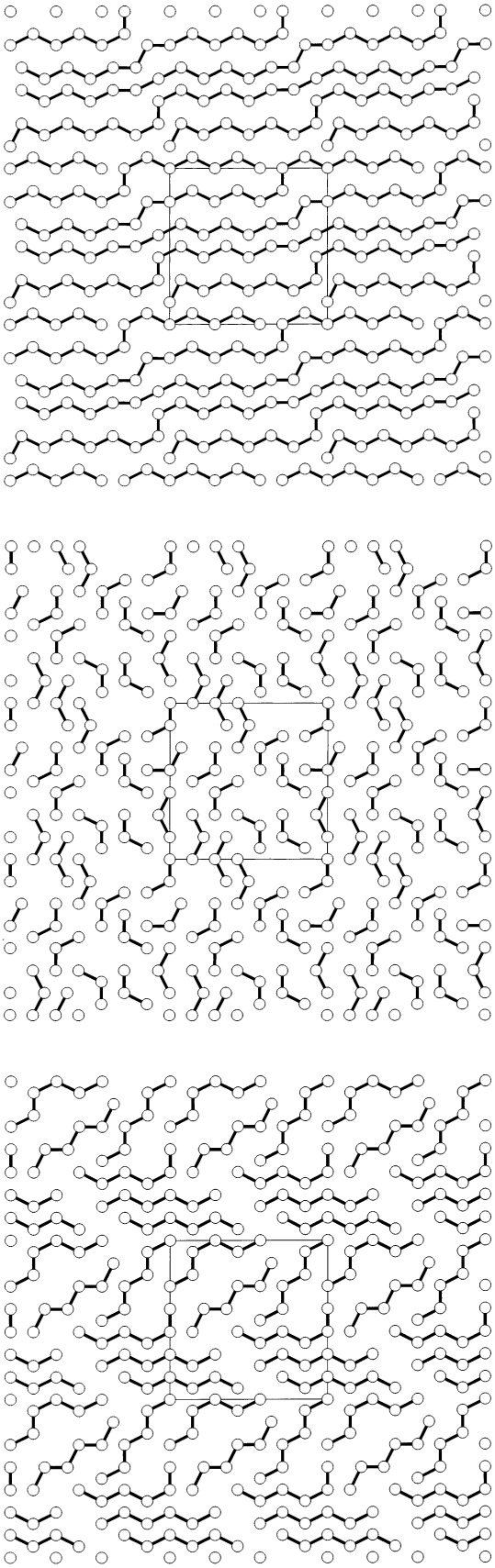

Figure 1. Minimum configurations of lattice polymers on a 14×14 lattice: (a) $N_p = 1$, $l_p = 36$; (b) $N_p = 12$, $l_p = 3$; (c) $N_p = 6$, $l_p = 6$. The $3 \times 3 = 9$ unit cells are shown. To avoid overloading the pictures, only the outline of the unit cell is given; the grid points of the underlying lattice are not included.

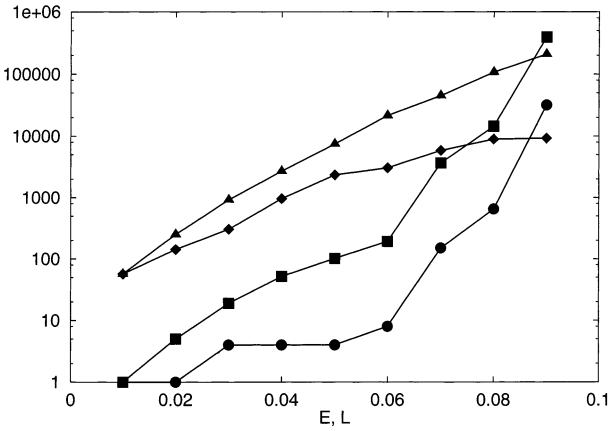

Figure 2. Number of accessible states $N(L)$ (squares), accessible minima $M(L)$ (circles), density of states $D(E;L = 0.09)$ (triangles), and density of minima $D_M(E;L = 0.09)$ (diamonds) per energy interval $\Delta E = 0.01$ eV/atom within a pocket as a function of L (eV/atom) and E (eV/atom), respectively, for a system of 2 polymers of length $l_p = 18$ on a 14 × 14 lattice.

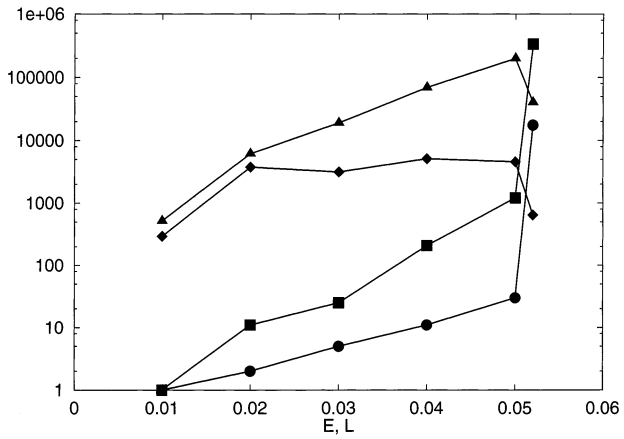

Figure 3. Number of accessible states $N(L)$ (squares), accessible minima $M(L)$ (circles), density of states $D(E;L = 0.052)$ (triangles), and density of minima $D_M(E;L = 0.052)$ (diamonds) per energy interval $\Delta E = 0.01$ eV/atom within a pocket as a function of L (eV/atom) and E (eV/atom), respectively, for a system of 12 polymers of length $l_p = 3$ on a 14 × 14 lattice. (The drop in $D(E;L = 0.052)$ and $D_M(E;L = 0.052)$ for $E = 0.052$ is a cutoff effect: the number of states for $L > 0.052$ exceeded the working memory capability of the computer (784 MB). Generating the data for this relatively small system required the equivalent of ca. 2 weeks on a DEC-α 433 MHz workstation.)

this was checked during the counting, and they were counted only once. Note that the lid algorithm is an exhaustive search procedure, in contrast to the closely related threshold algorithm,[37] which is based on a careful analysis of many random walks below a sequence of energy lids. Thus, we get a complete (but in a sense "static") picture of the local regions of the landscapes we investigate.

Results

The results show that while many properties of the pockets are common to all polymers considered, the polymers could be divided into two distinct classes, "long" polymers consisting of 10 or more building units and "short" polymers consisting of up to 6 building units. (Of the long polymers, 90% or more of the pockets exhibited "long-polymer"-like behavior, and similarly, over 90% of the short polymer pockets showed "short-polymer"-like behavior, respectively.) Polymers with lengths between exhibited behavior common to both, depending on the specific pocket considered. For the range of unit cells considered, this assignment to a given group did not depend on the size of the system V or the overall number density of building units $N_A/V = N_p l_p/V$.

In the description of the results, let us begin with the properties common to both classes of polymers. For simplicity, we always use the energy E_{min} of the deepest minimum in the pocket as the zero of the energy scale, $E_{min} = 0$. In all systems, the local densities of states $D(E;L)$ exhibited approximately exponential growth as a function of energy for fixed value of the lid L, $D(E;L) \propto \exp(\alpha_D E)$ (cf. Figures 2 and 3), where α_D indicates the rate of growth in $D(E;L)$. The same holds true for the density of minima $D_M(E;L)$ within a pocket, with the growth in the case of $D_M(E;L)$ being about equal or slightly slower than for $D(E;L)$, flattening for E close to the lid L. If one investigates the dependence of α_D on the size of the system, the number of building units, and the length of the polymers, one finds a more complex behavior than e.g. for the case of network glasses.[15,36] Nevertheless, some basic features can be distilled from the analysis: for a fixed density N_A/V and size V, α_D decreases slightly with increasing polymer length l_p. This is not unexpected, since small polymers tend to have slightly more freedom for minor readjustments. However, the major trends are analogous to those in two- and three-dimensional covalent networks:[15,36] increasing density for fixed volume decreases the rate of growth of $D(E;L)$, and increasing size for fixed density leads to a larger value of α_D.

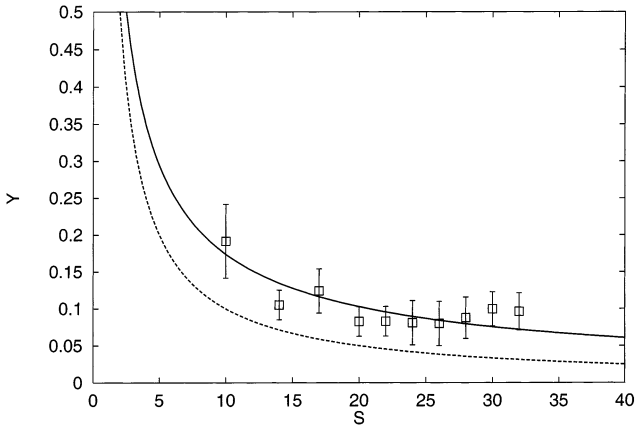

Figure 4. Plot of the product $Y = \langle E_i \rangle (1 - N_A V_A/V)$ of the inverse growth factor $\langle E_i \rangle$ averaged over all pockets i for polymers of a given number density $N_A/V = 0.18$ with the factor $(1 - N_A V_A/V)$ vs $S = V^{0.5}$ (cf. eq 4). The solid line shows the fit $f(V) = V^{-0.38}$. The curve that would correspond to the simple model (cf. eq 3), $f(V) = V^{-0.5}$, is shown as a dashed line.

Using a simple free-volume model that already successfully describes the dependence of α_D for 2D-covalent networks,[15] we find

$$\alpha_D = V^{1/2}(1 - V_A N_A/V) \qquad (3)$$

where V_A (=4) is the volume/atom in an ordered high-density ($\rho = \rho_{max} = 1/4$) state of the polymers. In contrast to the 2D-network glass ($\alpha_D \propto V$), in the case of 2D polymers the growth should be proportional to $V^{1/2}$, since the freedom of movement of the polymers is essentially restricted to moves perpendicular to the polymer backbone. (Quite generally, we find for a network in d dimensions $\alpha_D \propto V$, while for a polymer in d dimensions $\alpha_D \propto V^{(d-1)/d}$.) The polymers studied obey this rule only moderately well, as can be seen in Figure 4, where the product of the inverse rate of growth $\langle E_i \rangle$ (=$\langle 1/\alpha_i \rangle$) is averaged over all pockets i for long polymers ($l_p > 6$) of a given number density

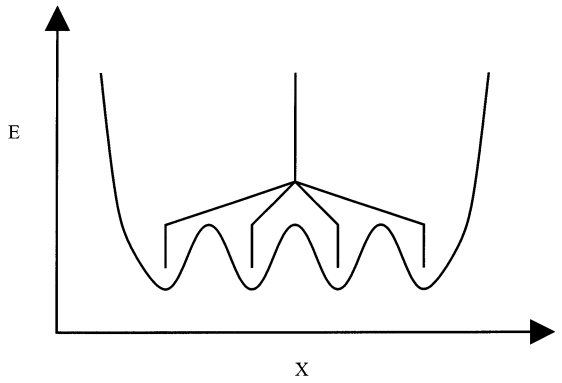

Figure 5. Schematic drawing of the landscape for small polymers, with corresponding lumped tree graph. The height of the barriers between the local minima corresponds to the energy E_c, above which the equivalent pockets of the landscape can communicate.

$N_A/V = 0.18$ and the factor $(1 - V_A N_A/V)$ is plotted vs $S = V^{0.5}$. [As mentioned above, short polymers do exhibit slightly faster rates of growth than long ones; e.g. for the shortest ones studied ($l_p = 3$), $\alpha_D(l_p = 3;S = 14) \approx 1.3\alpha_D(l_p = 18;S = 14)$. Thus, they were not included in the average in Figure 4, although their increase as function of system size V appears to follow eq 4 but probably with a slightly different value γ.] Assuming a simple power law

$$\langle E_i \rangle (1 - V_A N_A/V) \propto V^{\gamma} \tag{4}$$

we find for the best fit $\gamma = -0.38$. For comparison, we also plot the curve $f(V) = V^{-0.5}$, which would correspond to the simple parameter free model in eq 3.

The properties described above are shared by all polymer systems. The major difference between the two classes lies in the growth of the number of accessible states $N(L)$ and the general features of the barrier structure.

While for long polymers $N(L)$ grows smoothly exponentially, with the rate of growth α_N similar to the one of the local density of states α_D, for short polymers this exponential growth is interrupted by a large jump in $N(L)$ at some critical energy value L_C (cf. Figure 3). This value can actually be correlated with the energy that is needed in the system to allow for reptation-like movements of short polymers. Once this point has been reached, a large number of nearly equivalent configurations becomes accessible to the system. The fact that these newly accessible configurations are essentially equivalent can be deduced from a comparison of the density of states of the pocket $D(E;L < L_C)$ until $L = L_C$ (which closely parallels $N(L < L_C)$: $\alpha_N \approx \alpha_D$ for $L < L_C$) and $D(E;L > L_C)$. One finds that $D(E;L > L_C) \approx g(N_A,V)D(E;L < L_C)$, where g is the degeneracy of the ground state of the accessible region of the polymer system ($g = 10^2-10^4$, for the system sizes considered here). Note that despite this enormous enlargement of the accessible configuration space no deeper local minima are found. Thus, on this level, the energy landscape consists of a multitude of basically equivalent pockets that all join at a certain critical value $E_c = (E_{min} + L_C)$ of the energy barrier (cf. Figure 5).

In contrast (cf. Figure 2), the growth of $N(L)$ for long polymers exhibits no major jumps, beyond those that would be associated with the addition of a large subvalley as one is used from other complex systems such as the TSP[19] or covalent network glasses.[15] [The size of the jumps due to adding the phase space volume of one or more subvalleys depends on the number of states already present at the lid value. The relative increase in volume is the relevant quantity; pictorially, this is already implied in the logarithmic scale of plots of $N(L)$.] In particular, we find a considerably smaller degeneracy of the ground state within the accessible pocket ($g = 1-50$). Furthermore, the large side pockets join the main pocket at many different lids, and the overall shape of the density of states of these side pockets is similar to the main pocket though scaled down, of course. This is shown for a typical midsized pocket ($N(L) \approx 10^4$) in Figure 6. Thus, we do not deal with many nearly equivalent subpockets that join at some fixed energy barrier $E = E_c$. Instead, we encounter a hierarchy of barriers strongly reminiscent of analogous results for other complex systems.[19,36,38]

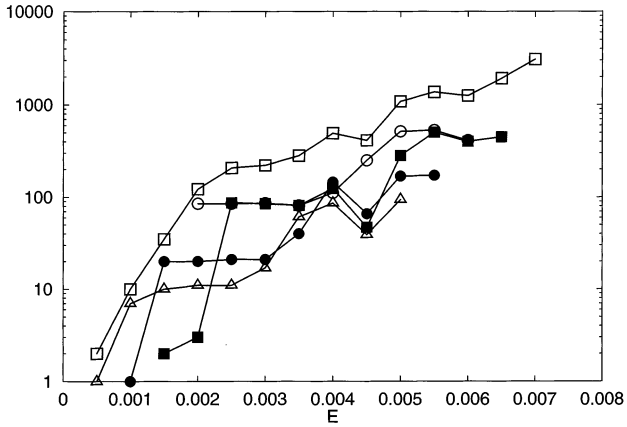

Figure 6. Plot of the density of states $D(E;L = 0.007)$ (hollow squares) per energy interval $\Delta E = 0.0005$ eV/atom for a midsize pocket in a system of 10 polymers of length 18 on a 32×32 lattice, together with the densities of states $D_i(E)$ of four substantial side pockets (hollow/full circles, full squares, hollow triangles) that join the main pocket at various energies. (The merging occurs at or right above the energy for the last data point of the side pocket's $D_i(E)$.) Note the overall similarity of the shape of the densities of states of the side pockets with the one belonging to the main pocket: a relatively sharp increase followed by a slower (average) growth. Due to the smaller size of the side pockets ($N_i(L_{max}) \approx 10^3$), the curves $D_i(E)$ are more jagged than $D(E)$ for the full pocket.

Discussion

The general consequences resulting from the approximately exponential growth of the local densities of states are shared by all polymer systems. In particular, they all show the typical metastable behavior caused by the existence of local exponential growth, which has already been discussed in detail in earlier work:[15,19,39] If $T > E_i$, the pocket will essentially be invisible despite its depth L; i.e., regarding the dynamics on the complex landscape as a whole, the probability that the system will enter the exponential traps is very small, since the number of low-lying states inside the trap is only an exponentially small fraction of the states located at the rim of the pocket. Thus, the system "floats" above them, essentially moving on a rather smooth "effective" landscape with comparatively small energy barriers. In contrast, for $T < E_i$, the system will reside somewhere at the bottom of the pocket in one of the many local minima, facing an energy barrier L it needs to cross before leaving the pocket; i.e., the system encounters the full very rugged landscape consisting of a multitude of traps of depth $L \gg E_i > T$. For this reason, E_i has been denoted the trapping temperature of the pocket. Thermodynamically, this behavior results in a peak in the specific heat near $T = E_i$ (cf. Figure 7), a behavior reminiscent of glasses.

However, the different features of the energy landscape for long and short polymers have important consequences for the

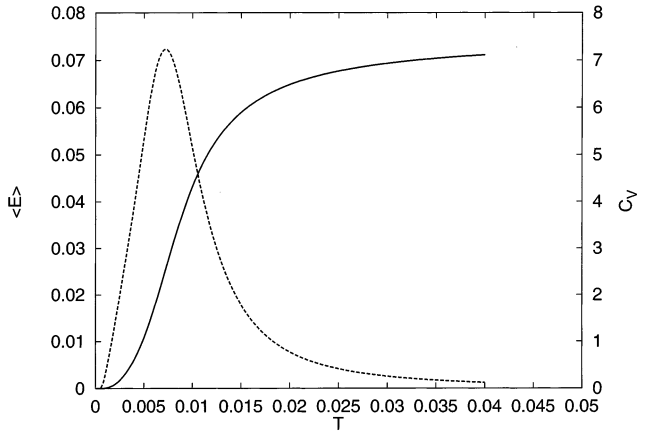

Figure 7. Plot of the expectation value of the energy $\langle E \rangle$ (eV/atom) (solid line) and the specific heat C_V (k_B) (dashed line) as a function of temperature T (eV/atom) for a large pocket belonging to a system of 2 polymers of length $l_p = 18$ on a 14×14 lattice (cf. Figure 2 for the density of states of the pocket). In this instance, the depth of the pocket $D \approx 0.09$ eV/atom exceeds the trapping temperature $E_i \approx 0.0093$ eV/atom by a factor of at least 10. Thus, for $T < E_i$, the system is trapped at the bottom of the pocket, as seen by the curve $\langle E \rangle(T)$. For $T \approx E_i$, the system moves to the top of the pocket, which gives rise to the peak in the specific heat. Note that $C_V(T)$ and $\langle E \rangle(T)$ have been calculated from the density of states restricted to the pocket, and thus they only describe the physics for $T \approx E_i$. For $T > E_i$ the system moves to the rim of the pocket and a much larger part of the landscape becomes accessible, and thus, e.g. $C_V(T)$ will not drop toward zero as shown but start increasing again at some point or reach some limiting value for $T > E_i$.

behavior of the polymer when crossing the trapping temperature. For long polymers, the analogy with e.g. 2D networks holds:[15] the exponentially growing pockets are large enough to act as traps ($D(E;L) \approx \exp(E/E_i)$ in the range of $0 \leq E \leq L$, with $L >> E_i$) and possess a (possibly self-similar) hierarchy of barriers B_{int}, the largest ones being comparable to the depth L of the pocket, $B_{int} \approx L$.

Furthermore, the trapping temperature E_i goes to zero as the system size V increases. Again, the fact that one nevertheless observes local equilibration in pockets for low temperatures suggests the following scenario: Beyond a certain system size, the pockets can become so large that due to the high internal ruggedness the equilibration time for the whole pocket exceeds the escape time from the pocket for temperatures close to E_i. [The escape time from the pockets is approximately $\tau_{esc} \approx \exp(L/T - L/E_i)$ for $T < E_i$, while the internal equilibration time of the pocket is controlled by the highest internal barriers (B_{int}) and the growth in the density of states of the individual subvalleys (characterized by E_{int}), together with the possibly labyrinthine structure of the rugged landscape in the pocket. Thus, we expect $\tau_{eq} > \exp(B_{int}/T - B_{int}/E_{int})$. Since in the long-polymer case, B_{int} is only slightly smaller than L and $E_{int} \approx E_i$, we expect that the equilibration time be approximately equal or even exceed the escape time, $\tau_{eq} \approx \tau_{esc}$, for $T \approx E_i$ for very large pockets.] As a consequence, on one hand the very large pocket as a whole can only achieve local equilibrium for T significantly below E_i, while on the other hand at least some, and perhaps the majority, of the subvalleys will lose metastability already at $T \approx E_{int} \geq E_i$ (cf. Figure 8). [This phenomenon that the accessible (locally equilibrated) phase space volume of a pocket can be considerably smaller than the pocket itself has also been observed during investigations of the energy landscape of MgF_2 with the threshold algorithm.[40]] This quantity E_{int} might well remain finite even as $E_i \rightarrow 0$, suggesting that even in the thermodynamic limit finite effective trapping

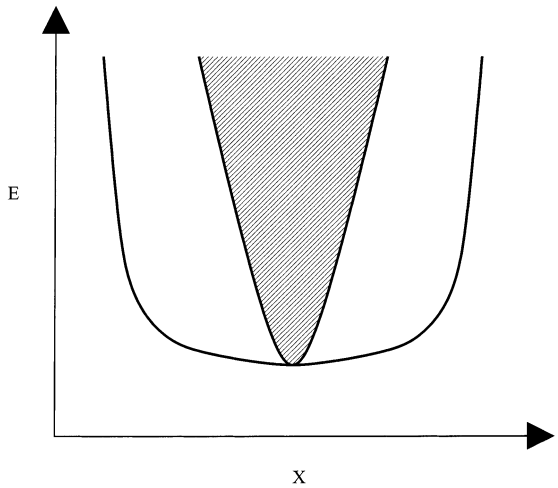

Figure 8. Schematic drawing of the fraction of a pocket (shaded) seen by a random walker out of equilibrium, resulting in an effective (quasi-equilibrium) density of states smaller than the actual one in the pocket. The time needed to equilibrate within the whole pocket is larger than the escape time τ_{esc} from the pocket. However, within the shaded region, the system is close to equilibrium for $t \ll \tau_{esc}$. The (possibly very complicated) internal energy barrier structure of the pocket that controls the size of the shaded region is not shown in this schematic, which stresses the accessible phase space volume.

temperatures might be present. [Note that we can use the simple model for $\alpha(V)$ represented above in eq 3 to estimate from the energy scales involved that a polymer system containing a few thousand building units should be large enough to reach the limit of local ergodicity and allow the modeling of many aspects of the glass transition, $T_g \approx E_i \approx 0.5$ eV for $N_A = 72$ ($V = 400$, $\rho = 0.72\rho_{max}$), and thus T_g will be in the realistic range of $\approx$0.05 eV for $N_A \approx 7000$. Of course, this estimate presupposes that trapping really constitutes a major contribution to the formation of glasses.]

In contrast, the short-polymer system partly evades the local equilibration issue, since enlarging the system size does not increase E_c and just increases $g(V)$. Thus while $D(E;L)$ overall increases, the change in its slope and the concomitant decrease in E_i is comparatively small and still follows approximately eq 3. Here, we need to distinguish between the increase in the number of individual polymers, which contribute to the decrease in E_i, and the increase in the number of equivalent subpockets. Clearly, since the local degrees of freedom of the individual polymers are only indirectly coupled to each other, the configuration space will again separate into weakly connected locally ergodic subspaces of a certain size.

But due to the splitting of the energy landscape into a multitude of equivalent subpockets, the behavior of the system takes place on several time scales: one for equilibration among many subpockets τ_1 (which for large subregions of the landscape cannot be done before leaving the whole pocket; cf. Figure 8) and one for equilibrating in a subpocket τ_2. But the fact that τ_1 grows quickly and soon exceeds the escape time for the whole subregion does not affect the short-polymer system in the same way as the large-polymer system, since the individual subpockets are essentially equivalent regarding their physical properties. Thus, it is τ_2 and not τ_1 that dominates the behavior as far as the overall physics is concerned! Furthermore, τ_2 does not increase as fast as τ_1 with growing system size, and due to the small size of these subpockets, ergodic barriers within the subpockets that in the end result in a finite value of the trapping temperature only appear after a considerable increase in total system size.

Thus, the short-polymer system exhibits a rapidly increasing number of equivalent locally ergodic regions, each with slowly but continually decreasing (identical) trapping temperatures, for increasing system size. Only when the barrier structures of these individual regions become complex enough does their ergodicity get broken and the trapping temperature reaches a finite limit value. But this takes place for much larger system sizes than for the long polymers, since short polymers interfere with each other much less than long polymers. A similar effect has been seen in MC−simulations of polymers of various lengths,[23] where an order of magnitude difference in cooling rates was needed to allow a $l_p = 10$ system to reach a similar low energy state as a $l_p = 3$ system. Conversely, we would have to impose a very high cooling rate to reach a disordered metastable configuration at low temperatures.

This type of behavior is much more like the one one would expect for a liquid than for a glassy state: except for very low temperatures, the system moves on the energy landscape well above the many local minima corresponding to possible (amorphous) structures ($T > E_i$!) without major potential energy barriers barring the way (except those that prevent large changes of the density of the system or the destruction of the individual polymers), leading e.g to a rather low viscosity. Note that, for a realistic system, the v.d.W.-intermolecular interactions between the individual polymers (which have been ignored in this analysis, to avoid the mixing of energy scales) need to be taken into account. Because of the energy barriers associated with the attraction between spatially close polymers, this interaction will also contribute to the viscosity and the solidification, of course. However the resulting formation of crystalline and/or glassy states on this energy level belongs more properly to the energy landscape of simple liquids, which is not part of this discussion, although it could also be analyzed using the lid algorithm.

Instead, we can perhaps draw an analogy to the liquid−nematic transition in liquid crystals.[41,42] The low-energy states of the lattice polymers presented here exhibit partly parallel arrangements of the individual chain molecules, with the (degenerate) ground state for a fixed density consisting of a perfectly parallel alignment of the polymers. Such an (on the average) aligned arrangement is also characteristic for the nematic phase and coincides with a loss of rotational symmetry in the system. But it is just this degree of freedom that is frozen out when the lattice polymers get trapped, while the further development toward more and more crystalline order only occurs if additional polymer−polymer interactions are taken into account. Furthermore, we note that liquid crystalline phases appear to be replaced by glassy phases once the length of the molecules involved exceeds some limit.[41] Again, this would qualitatively agree with our observations for the change of the behavior with polymer length in our model polymers.

Finally, recent studies of the crystallization of (essentially two-dimensional) polymers have shown ordered domains of aligned polymers or polymer sections of a characteristic size of 2−10 nm being formed during freezing.[43] Both the visual impression and the characteristic size of the domains are strongly reminiscent of the results presented here. The typical alignments in the local minimum configurations of the long-lattice polymers (cf. Figure 1) and the estimated size of the locally equilibrated domains of several thousand backbone-C atoms are both in qualitative and even semiquantitative agreement with these experimental observations.

While these results open up new and exciting avenues of investigation of polymers and related systems, we need to analyze which results are independent of the particular aspects of the model we have employed. Neglecting weak (van der Waals) interactions among the polymers leads to an artificial degeneracy of the minima of the system, including the ground state. Introducing such an interaction would lift this degeneracy to a certain extent, and e.g., the local minima sketched in Figure 5 would be shifted to slightly different energies. However, as long as this additional interaction is weak, the general statements and deductions about the pockets and their effect on the properties of the system would still apply.

A second issue is the use of a finite simulation cell. If we were to employ a very large cell, e.g. 100×100, we expect that even systems with long polymers such as $l_p = 18$ will exhibit many nearly equivalent arrangements resulting in very similar subregions of the landscape that are all connected above some critical energy value. Thus, the picture associated with Figure 5 would also apply for large polymers as long as the unit cell is big enough. However, the individual nearly equivalent subregions will be very large and retain their high internal complexity. Thus, we expect that their local structure will continue to control the thermodynamic behavior of the polymer, e.g. the existence or nonexistence of a glass transition. This expectation is supported by the observation that e.g. the properties of the pockets belonging to a system with 10 polymers of length 18 on a 32×32 lattice are still very similar to those belonging to a system consisting of one polymer of length 180 on the same lattice or those of 2 polymers of length 18 on a 14×14 lattice.

Finally, we would like to point to the other complex systems where such an exhaustive analysis of pockets of the energy landscape has been performed: spin glasses;[35,38] the traveling salesman problem (TSP);[19] 2D- and 3D-network glasses.[15,36] In all instances approximately exponentially growing local densities of states were observed that appear to be a general characteristic of such systems. The differences among these systems lie mainly in the details of the barrier structure: (self-similar) hierarchies for e.g. 2D-/3D-networks and long polymers contrasting multiple equivalent small pockets for e.g. short polymers. Exploring and classifying these structures should be a major goal for future investigations. In particular, it is also necessary to go beyond the simple single- or multiple-lump tree-graph models of energy landscapes[9,12,37,44,45] that have been created in the past for the description and analysis of continuous energy landscapes of polymers, clusters, and solids, if one wants to understand the influence of entropic barriers on the dynamics and thermodynamcis of complex systems.

Acknowledgment. I thank P. Sibani and G. Stollhoff for valuable discussions and K. Binder for a lucid introduction to lattice polymer models. Funding was kindly provided by the DFG via SFB408 and a habilitation stipend.

References and Notes

(1) Götze, W.; Sjögren, J. *Rep. Prog. Phys.* **1992**, *55*, 241.
(2) Jäckle, J. *Rep. Prog. Phys.* **1986**, *49*, 171.
(3) Ramakrishnan, T. V., Lakshmi, M. R., Eds. *Non-Debye Relaxation in Condensed Matter*; World Scientific: Singapore, 1987.
(4) Doi, M. *Introduction to polymer physics*; Clarendon Press: Oxford, U.K., 1997.
(5) Elliott, S. R. *Physics of Amorphous Materials*; Longman Scientific & Technical: Essex, U.K., 1990.
(6) Gutzow, I.; Schmelzer, J. *The Vitreous State*; Springer: Berlin, 1995.
(7) Fischer, K. H.; Hertz, J. A. *Spin glasses*; Cambridge University Press: Cambridge, U.K., 1991.
(8) Berry, R. S. *Chem. Rev.* **1993**, *93*, 2379.
(9) Wales, D. J.; Miller, M. A.; Walsh, T. R. *Nature* **1998**, *394*, 758.

(10) Wales, D. J.; Doye, J. P. K.; Miller, M. A.; Mortenson, P. N.; Walsh, T. R.. In *Advances in Chemical Physics*; Prigogine, I., Rice, S. A., Eds.; Wiley: New York, 2000; Vol. 115.
(11) Dill, K. A.; Bromberg, S.; Yue, K.; Fiebig, K. M.; Yee, D. P.; Thomas, P. D.; Chan, H. S. *Protein Sci.* **1995**, *4*, 561.
(12) Becker, O. M.; Karplus, M. *J. Chem. Phys.* **1997**, *106*, 1495.
(13) Becker, O. M. *J. Mol. Struct. (THEOCHEM)* **1997**, *398*−*399*, 507.
(14) Miller, M. A.; Wales, D. J. *J. Chem. Phys.* **1999**, *111*, 6610.
(15) Schön, J. C.; Sibani, P. *J. Phys. A: Math. Gen.* **1998**, *31*, 8167.
(16) Sibani, P.; Brandt, M.; Alstrom, P. *Int. J. Mod. Phys. B* **1998**, *12*, 361.
(17) Schön, J. C.; Jansen, M. *Angew. Chem., Int. Ed. Engl*. **1996**, *35*, 1286.
(18) Schön, J. C.; Jansen, M. *Z. Kristallogr*. **2001**, *216*, 307, 361.
(19) Sibani, P.; Schön, J. C.; Salamon, P.; Andersson, J.-O. *Europhys. Lett.* **1993**, *22*, 479.
(20) Kremer, K.; Binder, K. *Comput. Phys. Rep.* **1988**, *7*, 259.
(21) H. P. Wittmann, K. K.; Binder, K. *J. Chem. Phys.* **1992**, *96*, 6291.
(22) Binder, K. *Prog. Colloid Polym. Sci.* **1994**, *96*, 7.
(23) Lobe, B.; Baschnagel, J. *J. Chem. Phys.* **1994**, *101*, 1616.
(24) Binder, K.; Baschnagel, J.; Paul, W.; Wittmann, H. P.; Wolfgardt, M. *Comput. Mater. Sci.* **1995**, *4*, 309.
(25) Binder, K.; Baschnagel, J.; Bennemann, C.; Paul, W. *J. Phys.: Condens. Matter* **1999**, *11*, A47.
(26) Mai, J.; Sokolov, I. M.; Blumen, A. *J. Chem. Phys.* **1997**, *106*, 7829.
(27) Binder, K. *Comput. Phys. Commun.* **1999**, *122*, 168.
(28) Frauenfelder, H., Bishop, A. R., Garcia, A., Perelson, A., Schuster, P., Sherrington, D., Swart, P. J., Eds. Landscape Paradigms in Physics and Biology. *Physica D* **1996,** *107* (2−4).
(29) Schön, J. C. In *Proceedings of RIGI-workshop 1998*; Schreuer, J., Ed.; ETH Zürich: Zürich, 1998.
(30) Anderson, P. W.; Halperin, B. I.; Varma, C. M. *Philos. Mag.* **1972**, *25*, 1.
(31) Philipps, W. A. *J. Low-Temp. Phys.* **1972**, *7*, 351.
(32) Galperin, Y. M.; Gurevich, V. L.; Parshin, D. A. *Phys. Rev. B* **1985**, *32*, 6873.
(33) Buchenau, U.; Galperin, Y. M.; Gurevich, V. L.; Schober, H. R. *Phys. Rev. B* **1991**, *43*, 5039.
(34) Sibani, P.; v. d. Pas, R.; Schön, J. C. *Comput. Phys. Commun.* **1999**, *116*, 17.
(35) Sibani, P.; Schriver, P. *Phys. Rev. B* **1994**, *49*, 6667.
(36) Schön, J. C.; Sibani, P. *Europhys. Lett.* **2000**, *49*, 196.
(37) Schön, J. C. *Ber. Bunsen-Ges. Phys. Chem.* **1996**, *100*, 1388.
(38) Sibani, P. *Physica A* **1998**, *258*, 249.
(39) Schön, J. C. *J. Phys. A: Math. Gen.* **1997**, *30*, 2367.
(40) Wevers, M. A. C.; Schön, J. C.; Jansen, M. *J. Phys.: Condens. Matter* **1999**, *11*, 6487.
(41) Demus, D. *Mol. Cryst. Liq. Cryst.* **2001**, *364*, 25.
(42) Gennes, P. G. D.; Prost, J. *The Physics of Liquid Crystals;* Oxford Science: Oxford, U.K., 1993.
(43) Percec, V.; et al. *J. Am. Chem. Soc.* **1998**, *120*, 8619.
(44) Hoffmann, K. H.; Sibani, P. *Phys. Rev. A* **1988**, *38*, 4261.
(45) Heuer, A. *Phys. Rev. Lett.* **1997**, *78*, 4051.